Postharvest Biology and Technology 219 (2025) 113266

Contents lists available at ScienceDirect

Postharvest Biology and Technology

journal homepage: www.elsevier.com/locate/postharvbio

UV-B radiation mitigates oxidative stress damage in postharvest *Agaricus bisporus* by modulating the antioxidant defense system

Xueli Shang [a], Shiqi Bai [a], Liang Wen [b], Alfred Mugambi Mariga [c], Ning Ma [a], Donglu Fang [d], Wenjian Yang [a], Qiuhui Hu [a], Fei Pei [a,*]

[a] College of Food Science and Engineering, Nanjing University of Finance and Economics/Collaborative Innovation Center for Modern Grain Circulation and Safety/ Jiangsu Province Engineering Research Center of Edible Fungus Preservation and Intensive Processing, Nanjing 210023, China
[b] Information Center of Shenzhen Customs, Shenzhen 518045, China
[c] School of Agriculture and Food Science, Meru University of Science and Technology, Meru County P.O Box 972-60200, Kenya
[d] Department of Food Science and Technology, College of Light Industry and Food Engineering, Nanjing Forestry University, Nanjing 210037, China

ARTICLE INFO

Keywords:
ROS metabolism
Peroxisome homeostasis
Ascorbate-glutathione
UV Resistance Loucs 8

ABSTRACT

Agaricus bisporus (*A. bisporus*) has fragile tissues and is highly susceptible to post-harvest decay and spoilage, which affecting the development of the industry. Ultraviolet B (UV-B) irradiation, as a typical irradiation preservation technology, is effective in inducing the production of endogenous metabolic substances in organisms and enhancing their level of resistance. The objective of this study was to investigate the mechanism of activation of the antioxidant defence system in *A. bisporus* by UV-B irradiation, utilising a range of UV-B irradiation doses (0, 25, 50 and 100 kJ m^{-2}). In this study we found that 50 kJ m^{-2} UV-B irradiation effectively delayed the accumulation of reactive oxygen species (ROS), inhibited NADPH oxidase (NOX) activity and the expression of *Rbohf*, *PXMP2*, *PXMP4*, *APO*, and *MPV17*. Moreover, it could increase the accumulation of ascorbate (AsA) and glutathione (GSH), enhance the activities of ascorbate peroxidase (APX) and glutathione peroxidase (GSH-PX), and it also effectively induce catalase (CAT), superoxide dismutase (SOD) and peroxidase (POD) activities and up-regulate the expression levels of related genes. In addition, we found that UV-B irradiation upregulated the expression of *UVR8* and suppressed the expression of *PEX5*, *PEX11* and *PMD1*. These results suggest that 50 kJ m^{-2} UV-B irradiation could stimulate the UV Resistance Loucs 8 (UVR8) receptor, regulate peroxisome proliferation, and enhance the ability of *A. bisporus* to resist oxidative stress, thereby maintaining the cellular redox homeostasis, this provides a new strategy for the study of extended postharvest storage stability of *A. bisporus*.

1. Introduction

Agaricus bisporus (*A. bisporus*) are popular by consumers due to high nutritional value, which is rich in protein and it also contains vitamins, soluble sugar, polyols, free amino acids and other nutrients, as well as unique aroma and flavor. However it is easy to be physically or microbiologically damaged, and the skin starts to brown, the cap opens veil, and eventually the fruiting body rots and deteriorates, which seriously affects its commercial value due to its high moisture content, high respiration rate and lack of cuticle protection (Dokhanieh and Aghdam, 2016; Zhang et al., 2018). Therefore, it is crucial for the development of *A. bisporus* industry through the study of suitable preservation techniques.

Rapid accumulation of reactive oxygen species (ROS) is a typical oxidative stress response in postharvest *A. bisporus* and it's also a key factor causing its quality deterioration, which mainly includes hydrogen peroxide (H_2O_2) and superoxide anion radical ($O_2^{\bullet-}$). Early ROS generated through the NADPH oxidase (NOX) pathway act as signaling molecules to activate antioxidant system-related metabolism (Lin et al., 2024). Meanwhile, the imbalance of physiological metabolism and the weakening of antioxidant capacity led to the accumulation of ROS during the storage of *A. bisporus*, which in turn led to protein and DNA damage, membrane lipid peroxidation and destruction of cellular structure, and ultimately to quality deterioration such as browning, stickiness, and umbrella opening (Liu et al., 2013). Therefore, the inhibition of ROS accumulation and elimination of excessive ROS in

* Corresponding author.
E-mail address: feipei87@163.com (F. Pei).

https://doi.org/10.1016/j.postharvbio.2024.113266
Received 21 August 2024; Received in revised form 20 September 2024; Accepted 12 October 2024
Available online 19 October 2024

postharvest *A. bisporus* is the key to delay oxidative damage.

Ultraviolet-B (UV-B) is a medium wave ultraviolet light (280–315 nm) that not only has excellent bactericidal effects, but is also important for maintaining the quality of postharvest fruits and vegetables by activating defense system (Usall et al., 2016). The proper doses of UV-B radiation have been reported to be ecologically important in regulating the growth and development of many plants, whereas high doses of UV-B may cause damage to plants at the cellular and molecular levels (Zhang et al., 2023; Shoaib et al., 2024). When faced with UV-B radiation, organism activate various mechanisms to prevent or mitigate the ensuing oxidative damage. It was found that UV-B exposure induces the production of antioxidant substances such as ascorbic acid, phenols, flavonoids (Vidović et al., 2015). Li et al. (2021) found that proper UV-B pre-irradiation promoted polyphenol accumulation and maintained blueberry quality. Santin et al. (2018) found through their study that postharvest UV-B radiation could regulate metabolites in peach fruits thereby inducing phenolic accumulation. In addition, UV-B can eliminate excess ROS in the organism by activating antioxidant enzymes such as catalase (CAT), superoxide dismutase (SOD). Wu et al. (2021) found that postharvest UV-B radiation increased antioxidant enzyme activity in honeysuckle.

A lot of studies have found UV-B to be effective in improving postharvest quality and prolonging shelf life of fruits and vegetables. However, the molecular mechanism of UV-B irradiation on the quality enhancement is still unclear. In this study, we investigated the effects of UV-B irradiation on the key pathways of peroxisomal antioxidant defense and ROS metabolism by irradiating postharvest *A. bisporus* with different dosages of UV-B irradiation, with the aim of providing theoretical basis for the technology of retarding quality deterioration of postharvest *A. bisporus*.

2. Material and methods

2.1. Pre-treatment for UV-B irradiation

Fresh *A. bisporus* were purchased from market (Wuhe Zhongxing Mushroom Technology Co., Ltd.) and transported to the laboratory under refrigeration. Samples of the same size and without external damage were selected and randomly divided into four groups of twenty mushrooms each. The method of Sheng et al. (2018) was employed for the requisite adjustments. UV-B irradiation is performed using a UV-B lamp (PHILIPS TL 20 W/12 RS) approximately 0.75 m in length. *A. bisporus* that require irradiation were positioned in a uniform manner beneath the lamp, and the irradiation dose was regulated by the irradiation time to be 0 kJ m^{-2}, 25 kJ m^{-2}, 50 kJ $m^{-2}$and 100 kJ m^{-2}. The intensity of UV irradiation at different locations under the lamp is monitored in real time using a UV-irradiometer (Shenzhen Lianhuicheng Technology Co., Ltd.) to ensure uniformity of irradiation. 0 kJ m^{-2} treatment group without UV-B irradiation treatment, the irradiation times for the 25 kJ m^{-2}, 50 kJ m^{-2} and 100 kJ m^{-2} groups were 47 min, 92 min and 184 min, respectively. After completion, all samples were stored in a constant temperature and humidity chamber (4°C and 90 % relative humidity) for 18 days. Samples were taken from each group every three days during the storage period, measured and analyzed.

2.2. Appearance and browning determination

The color of *A.bisporus* mushroom cap surface was measured by colorimeter. Three points were randomly selected for each mushroom cap to measure L*, a* and b* of *A.bisporus*, and the total color difference change of *A.bisporus* was reflected by ΔE, which was calculated as follows.

$$\Delta E = \sqrt{(L^* - 97)^2 + (a^* - (-2))^2 + b^{*2}} \quad (2.1)$$

Browning index (BI) represents the degree of browning of *A.bisporus* and was calculated as follows.

$$\chi = \frac{a^* + 1.75L^*}{5.645L^* + a^* - 3.102b^*} \quad (2.2)$$

$$BI = \frac{100(\chi - 0.31)}{0.172} \quad (2.3)$$

2.3. Determination of ROS content and observation of distribution

$O_2^{\bullet -}$ content was determined according to the instruction manual of the kit (Beijing Solarbio Science & Technology Co., Ltd.) and calculated and expressed as mmol kg^{-1}.

H_2O_2 content was determined according to the kit instructions and (Beijing Solarbio Science & Technology Co., Ltd.), calculated and expressed as mol kg^{-1}.

Fresh *A. bisporus* were cut into pieces and dripped with the embedding agent OCT, pre-cooled, trimmed and pasted on the embedding table, quick-frozen and embedded, and then sliced when they turned white and hardened. The embedded blocks were fixed on the sectioning table, cut into 4 μm thick slices along the cross-section, pasted on slides, and controlled to dry. The slides were treated with autofluorescence quencher for 5 min and rinsed under running water for a further 10 min. The ROS staining solution was added dropwise to the sections and incubated for 30 min at 37°C in a dark environment. After incubation, the slides were placed in phosphate buffer (pH 7.4) and washed 3 times for 5 min each by shaking on a shaker. Subsequently, the sections were dehydrated and the coverslips were then coated on one side with an anti-fluorescence quenching sealer. The images were collected by laser confocal microscope (LSCM, FLUOVIEW FV1200, Olympus, Japan) with excitation wavelength of 510–560 nm and emission wavelength of 590 nm.

2.4. NOX activity measurement

The activity of NOX was determined according to the NADPH-OX kit instructions (Shanghai Enzyme-linked Biotechnology Co., Ltd.). The absorbance at 450 nm was measured and the NOX activity was calculated.

2.5. Measurement of AsA and GSH content

Ascorbate (AsA) content was determined according to the instruction of the kit (Nanjing Jiancheng Biotechnology Research Institute Co., Ltd.). The AsA content in *A. bisporus* was calculated and expressed as g kg^{-1}.

Glutathione (GSH) content was determined according to the instruction of the kit (Nanjing Jiancheng Biotechnology Research Institute Co., Ltd.). The GSH content in *A. bisporus* was calculated and expressed as g kg^{-1}.

2.6. Measurement of CAT, SOD, POD, APX and GSH-PX activity

The activity of CAT was determined according to the kit instructions (Beijing Solarbio Science & Technology Co., Ltd.). One unit (U) of CAT was defined as one unit of activity per gram of tissue decomposing 1 μmol of H_2O_2 per second. CAT activity in *A. bisporus* was calculated and expressed as U kg^{-1}.

The activity of SOD was determined according to the kit instructions (Beijing Solarbio Science & Technology Co., Ltd.). Definition of SOD enzyme viability unit: SOD enzyme viability in the xanthine oxidase coupling system was defined as one enzyme viability unit (U) at 50 % inhibition in the reaction system. SOD activity in *A. bisporus* was calculated and expressed as U kg^{-1}.

The activity of peroxidase (POD) was determined according to the kit instructions (Beijing Solarbio Science & Technology Co., Ltd.). One unit

(U) of POD was defined as 0.005 per g of tissue per minute A470 nm change per mL of reaction system. POD activity in *A. bisporus* was calculated and expressed as U kg^{-1}.

The activity of ascorbate peroxidase (APX) was determined according to the kit instructions (Beijing Solarbio Science & Technology Co., Ltd.). One unit of activity (U) of APX was defined as one unit of enzyme activity per gram of tissue catalyzing 1 μmol of AsA per minute per mL of reaction system. APX activity in *A. bisporus* was calculated and expressed as U kg^{-1}.

The activity of glutathione peroxidase (GSH-PX) was determined according to the kit instructions (Beijing Solarbio Science & Technology Co., Ltd.). One unit of GSH-PX activity (U) was specified as one unit of enzyme activity per milligram of tissue that reduced the GSH concentration in the reaction system by 1 μmol L^{-1}. GSH-PX activity in *A. bisporus* was calculated and expressed as U kg^{-1}.

2.7. Real-time fluorescence gene expression assay

RNA was extracted using the Fungal RNA kit (Vazyme Biotech Co., Ltd), and RNA concentration was determined using an ultra-micro spectrophotometer, with a blank control of ddH_2O and a sample volume of 3 μL. RNA was reverse transcribed to cDNA by HiScript lll RT SuperMix for qPCR (+gDNA wiper) for use. Relative gene expression was detected according to the Taq Pro Universal SYBR qPCR Master Mix instructions. 2x Taq Pro Universal SYBR qPCR Master Mix, 10 μM Primer, cDNA, ddH_2O mix was configured in a qPCR tube and underwent a pre-denaturation at 95°C for 30 s. Subsequently, the qPCR tube was subjected to 40 cycles of cyclic reactions at 95°C for 10 s and 60°C for 30 s, finally one cycle of 95°C for 15 s, 60°C for 60 s 95°C for 15 s was performed for the melt curve acquisition phase. The reaction Ct values were recorded according to the 2 Taq Pro Universal SYBR qPCR Master Mix, 10 μM Primer, cDNA, ddH_2O mix, and the relative expression of the target gene mRNA was calculated according to the $2^{-\Delta\Delta Ct}$ formula. The internal reference gene was *Gapdh*, primers were designed on NCBI and synthesized by Sangon Bioengineering (Shanghai) Co, Ltd, the gene sequences are shown in Table 1.

Table 1
The primer sequences for quantitative real-time PCR.

Gene name	Primer sequences (5'-3')
Gapdh	F: TCACGCCACCACCGCTACTCAA
	R: CGGGCTTCTCAAGACGAACAACAA
Rbohf	F: CGTCCACCTTACTGCTCATACAAC
	R: CAATCCAGATGACACCACCGATAAG
PXMP2	F: AGCTAATTGTACGCACGCAGAC
	R: CATCTTTCTTCGCCTTCTCCTTCTC
PXMP4	F: TAGACTCATCTGCCGTTCCTTCC
	R: TGCGTGCTCCCTTTAGAATTGC
MPV17	F: TCTCATCGCAAATTGGAAGGTCTG
	R: TGGGTAAATGGAACTCGGTAGGG
APO	F: CATGGCGATAACTGGCAATTCAAC
	R: TCAGCGAACTTTGGCAAGGTAAG
CAT2	F: CGAACAACTCCAGCAGGGTTTAATC
	R: TGAGGTCAAGATCATCGGTGAGAAG
SODc	F: TGCGGTGGGTCTCATTGTCTTC
	R: ATCACACCACATGCGACTCTAGC
PrxQ	F: ATTGATTCCGAGTGCGTGATTAGAG
	R: TCACTGCTAAGCCTCCGACTTC
UVR8	F: TCCGTTGAGTGAGATACCTGAAGG
	R: ACTCCGCTCGTTGCCTCTTG
PEX5	F: TGAATGTGGATCAAGGTGCTGTTC
	R: TGAATGTGGATCAAGGTGCTGTTC
PEX11	F: AGACAGTCAGGCTCAACGAGGAG
	R: GCGGCAAGGGCACTCAGTTTAG
PMD1	F: CCATTTCAATGTCACGAAGCAAAGC
	R: TCCGTTGTTTCTCTCCACCACTG

2.8. Statistical analysis

All determination was done at least three times. Datas were expressed as means ± standard errors (SE). One-way analysis of variance (ANOVA) was performed using IBM SPSS Statistics 26.0 software, and significant differences between the two groups were determined using Duncan's test. Differences at $P < 0.05$ was considered statistically significant.

3. Results

3.1. Effect of different doses of UV-B irradiation on the appearance and browning degree

The changes in the appearance of *A.bisporus* after UV-B irradiation at different doses during the storage period are shown in Fig. 1A. It can be found that 100 kJ m^{-2} irradiation dose caused a slight browning and yellowing of the cap surface. From D9 onwards, the appearance of the treatment groups differed, with the 0 kJ m^{-2} and 25 kJ m^{-2} groups showing brown spots. At D12, the browning of the 0 kJ m^{-2} and 25 kJ m^{-2} groups deepened, the surface browning of the 100 kJ m^{-2} group intensified, and the overall appearance of the 50 kJ m^{-2} group was better. At D18, the control group showed large brown patches and almost lost its commercial value, the 25 kJ m^{-2} group showed more brown spots, the 100 kJ m^{-2} irradiated group showed more browning, and the 50 kJ m^{-2} irradiated group showed only a slight yellowing of the cap. In contrast, the browning degree of *A.bisporus* in the 50 kJ m^{-2} UV-irradiated group was the smallest, indicating that the irradiation dose of 50 kJ m^{-2} was effective in inhibiting the browning of *A.bisporus* after harvesting and reducing the quality deterioration.

In addition, it can be observed that the L* of the samples decreased continuously during the storage period (Fig. 1B), whereas both L* and BI increased (Fig. 1C-D). The color difference values of the four groups of samples differed from D9 onwards, which is consistent with the appearance results. While 50 kJ m^{-2} could maintain a low and BI until D18, which is consistent with the good appearance maintained in the previous section.

3.2. Effects of different doses of UV-B irradiation on the distribution and content of ROS in A. bisporus

The distribution of ROS, $O_2^{\bullet-}$ content and H_2O_2 content of *A. bisporus* mushrooms after harvesting with different doses of UV-B irradiation are shown in Fig. 2. The ROS content increased with the increase of storage time. After D6, differences were directly observed in different treatment groups, and the H_2O_2 content of the 50 kJ m^{-2} group was lower than that of the other groups. At D18, the H_2O_2 contents of 0 kJ m^{-2}, 25 kJ m^{-2}, 50 kJ m^{-2} and 100 kJ m^{-2} treatment groups were 0.27 mol kg^{-1}, 0.28 mol kg^{-1}, 0.21 mol kg^{-1}, 0.28 mol kg^{-1}, respectively. Similarly, the $O_2^{\bullet-}$ content also increased with storage time, and it could be found that the $O_2^{\bullet-}$ content of the 50 kJ m^{-2} group was lower than that of the CK group from D9, and at D18, the $O_2^{\bullet-}$ content of the 0 kJ m^{-2}, 25 kJ m^{-2}, 50 kJ m^{-2} and 100 kJ m^{-2} treatment groups was 0.30 mmol kg^{-1}, 0.30 mmol kg^{-1}, 0.25 mmol kg^{-1}, and 0.30 mmol kg^{-1}, respectively. These data suggest that 50 kJ m^{-2} UV-B irradiation treatment can effectively delay ROS accumulation in postharvest *A. bisporus*, which may be due to the UV-B induced the ROS scavenging system and reduced ROS accumulation in the organism (Yokawa and Baluška, 2015).

3.3. Effect of different doses of UV-B irradiation on activity of NOX and gene expression of Rbohf

NOX is also known as respiratory burst oxidase homolog (RBOH), is an important potential enzymatic source of ROS during the oxidative burst (Chapman et al., 2019). NOX is responsible for $O_2^{\bullet-}$ production,

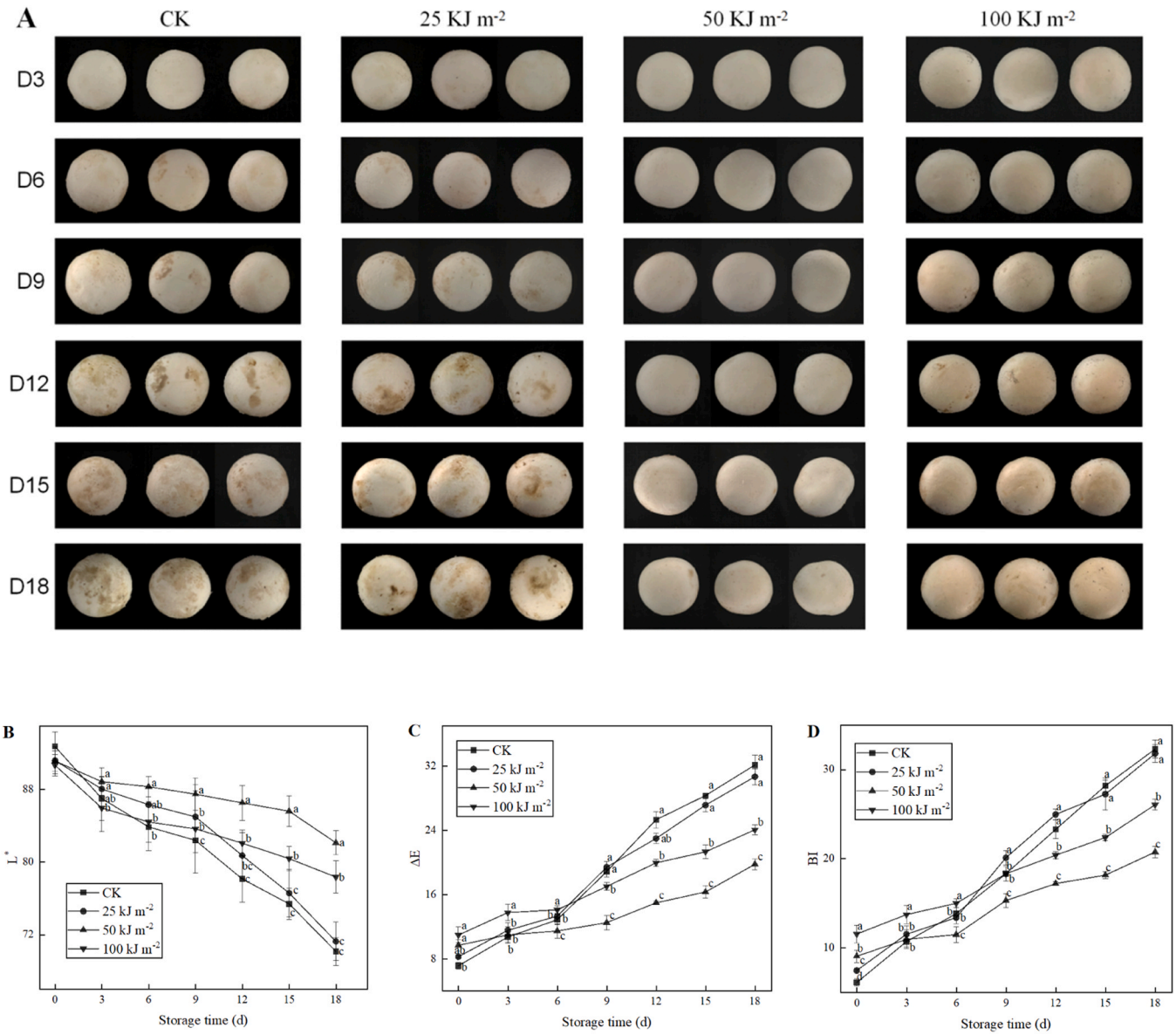

Fig. 1. Effect of different doses of UV-B irradiation on the appearance of *A. bisporus* (A), L* (B), ΔE (C), BI (D). Dates are expressed as mean ± SD (n = 3). According to Duncan's multiple range test, different lowercase letters indicate significant differences between different treatment groups for the same storage period ($P < 0.05$).

and NOX is activated by various cellular stresses such as chemical factors, cellular stimuli, or UV irradiation, etc (Wang et al., 2016). A study by Glady et al. (2018) found that knockdown of *Nox1* inhibited UV-B-induced p38 activation, suggesting that NOX may be involved in UV-B-induced intracellular signaling.

Through Fig. 3A, it can be found that NOX activity decreased continuously from D3 to D9, and has been increasing since then, reaching a peak at D18, with four groups of enzyme activities of 159.93 U kg^{-1}, 170.80 U kg^{-1}, 108.62 U kg^{-1}, and 121.81 U kg^{-1}, respectively. At D0, the 50 kJ m^{-2} and 100 kJ m^{-2} groups of NOX activity was higher than in the CK group, which may be influenced by the oxidative stress generated in the organism due to UV-B irradiation stress. From D3 onwards, the NOX activity of the 50 kJ m^{-2}-treated group was lower than that of the control group over time, while the relative expression of *Rbohf* in the 50 kJ m^{-2}-treated group was

lower than that of the control group and the other treatment groups (Fig. 3B). These results indicated that 50 kJ m^{-2} UV-B irradiation had a more pronounced inhibitory effect on NOX activity and gene expression thereby reducing the accumulation of ROS in the membrane.

3.4. Effects of different doses of UV-B irradiation on the peroxisomal ROS metabolic pathway

The relative expression of *PXMP2* and *PXMP4* in different irradiation treatment groups during storage is shown in Fig. 4A and Fig. 4B, which peaked at D9 and D12, respectively, and the 50 kJ m^{-2} irradiation group exhibited lower expression levels of *PXMP2* and *PXMP4* throughout the storage period relative to the other three groups. This suggests that less H_2O_2 produced by the peroxisome of *A. bisporus* passes through the PXMP2, PXMP4 pathway after being subjected to 50 kJ m^{-2} UV-B irradiation stress.

It can be observed that the relative expression level of *MPV17* increases and the relative expression level of *APO* decreases in *A. bisporus* after UV-B irradiation stress. During the entire storage period, the expression level of *MPV17* first decreased and then increased, with the 50 kJ m^{-2} irradiation group lower than the CK group (Fig. 4C and Fig. 4D). At D15, the expression of *MPV17* reached 1.28 in the CK group and 1.02 in the 50 kJ m^{-2} group, suggesting that 50 kJ m^{-2} UV-B irradiation may have retarded peroxisomal ROS metabolism.

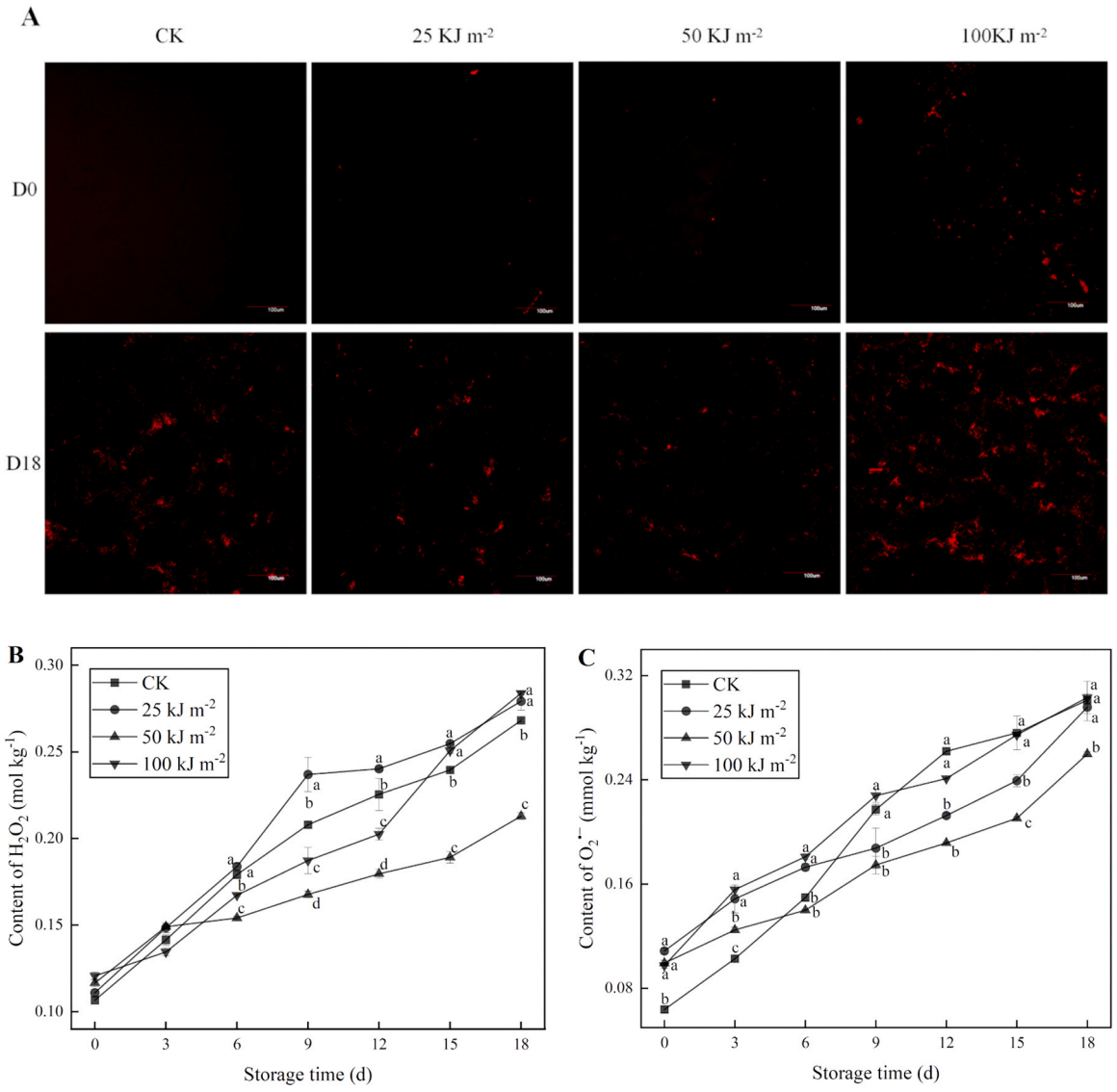

Fig. 2. Effect of different doses of UV-B on ROS distribution (A), H_2O_2 content (B) and $O_2^{\bullet-}$content (C) and relative expression of *UVR8* (D) in *A. bisporus*. Dates are expressed as mean ± SD (n = 3). According to Duncan's multiple range test, different lowercase letters indicate significant differences between different treatment groups for the same storage period ($P < 0.05$).

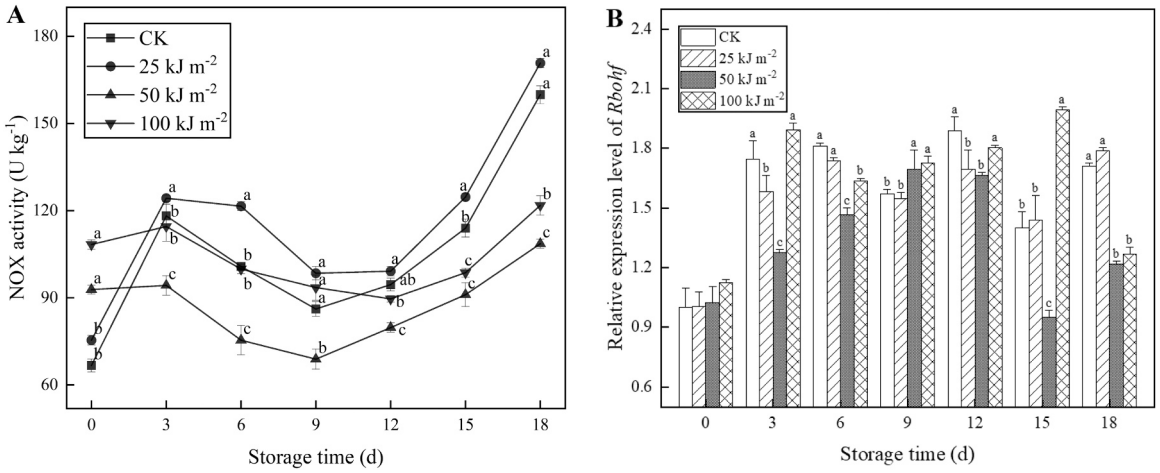

Fig. 3. Effect of different doses of UV-B irradiation on NOX (A), *Rbohf* (B)in *A. bisporus.* Dates are expressed as mean ± SD (n = 3). According to Duncan's multiple range test, different lowercase letters indicate significant differences between different treatment groups for the same storage period ($P < 0.05$).

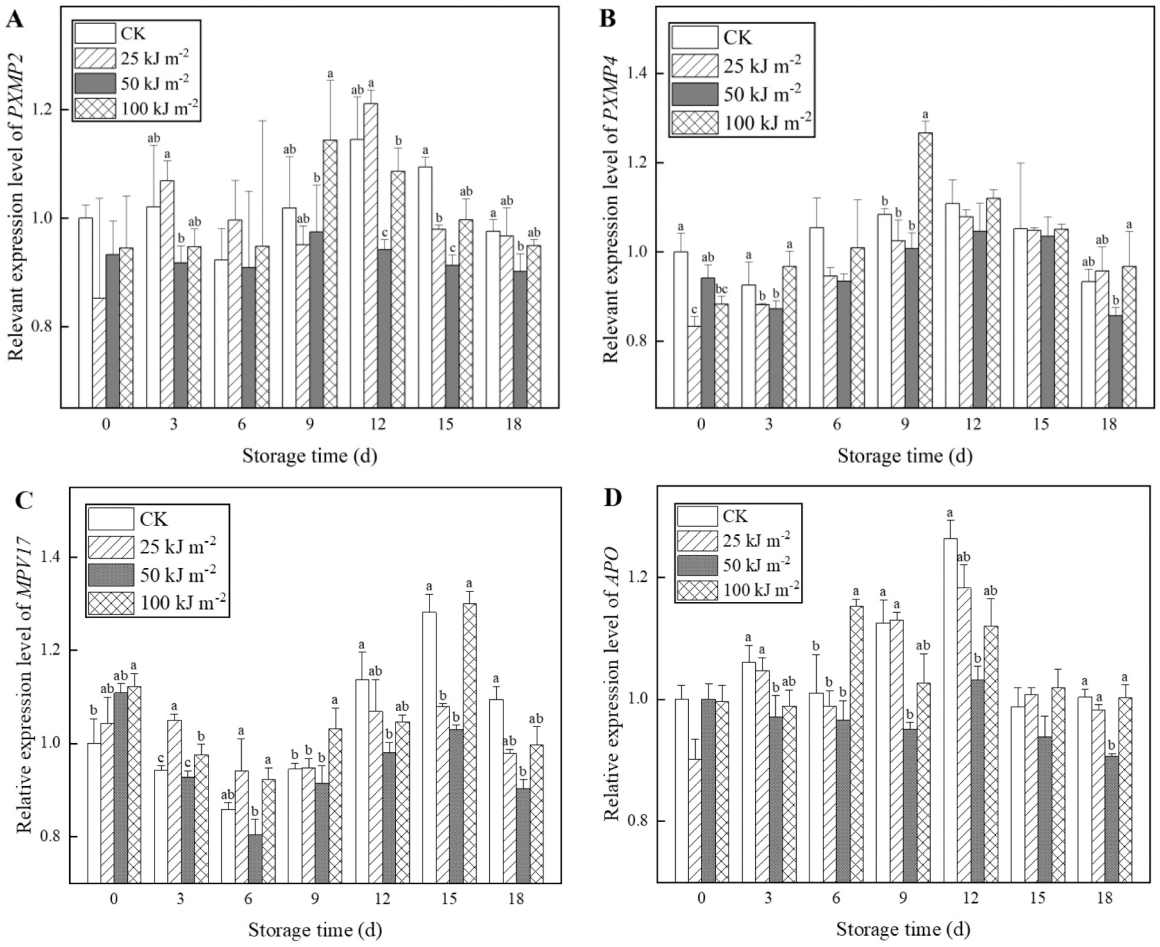

Fig. 4. Effect of different doses of UV-B irradiation on the enzyme activities of CAT (A), SOD (B), POD (C) and the relative expression of *CAT2* (D), *SODc* (E) and *Prxq* (F) in *A. bisporus*. Dates are expressed as mean ± SD (n = 3). According to Duncan's multiple range test, different lowercase letters indicate significant differences between different treatment groups for the same storage period ($P < 0.05$).

3.5. Effects of different doses of UV-B irradiation on AsA and GSH content and APX and GSH-PX activities

Fig. 5A shows the trend of AsA content during storage. The AsA content decreased continuously at the beginning of storage, and the four groups of content decreased from 0.90 g kg^{-1}, 1.05 g kg^{-1}, 1.10 g kg^{-1}, and 0.92 g kg^{-1} to 0.80 g kg^{-1}, 0.87 g kg^{-1}, 0.89 g kg^{-1} and 0.72 g kg^{-1} respectively, and then increased, which may be due to backfilling of monodehydroascorbic acid (MDHA) (Hasanuzzaman et al., 2018). The levels peaked again at D12 and remained high throughout the storage period in the 50 kJ m^{-2} UV-B irradiation treated group, and at D18, the AsA level in the 50 kJ m^{-2} irradiation treated group was 20 % higher than that of the control group.

Fig. 5B shows the trend of changes in APX during storage. There was an increasing trend of APX content from D0 to D15, with a maximum at D15. The APX content of the four treatment groups was 15.56 × 10^3 U kg^{-1}、15.36 × 10^3 U kg^{-1}、17.51 × 10^3 U $kg^{-1}$and 15.88 × 10^3 U kg^{-1} respectively, 50 kJ m^{-2} UV-B irradiation treatment group was higher than the other groups during storage.

Fig. 5C shows that the levels of glutathione content varied among the different treatments and control groups. The GSH content increased with the increase of storage time and reached the maximum peak at D15, with the levels of 36.42 g kg^{-1}, 40.81 g kg^{-1}, 46.36 g kg^{-1}, and 39.39 g kg^{-1} for the four groups, respectively. 50 kJ m^{-2} UV-B irradiation treatment group was higher than the other groups during storage, and at D18 the level of glutathione was 20 % ($P < 0.05$) higher in the 50 kJ m^{-2} irradiated group was 66.42 %, 23.17 % and 10.83 % higher than the control group, 25 kJ m^{-2} and 100 kJ m^{-2}, respectively.

Fig. 5D shows a trend of increasing and then decreasing changes in GSH-PX , and reaches its maximum value at D12, the APX content was 47.52 U kg^{-1}、46.95 U kg^{-1}、51.48 U kg^{-1} and 47.93 U kg^{-1}, respectively. From D9 to D18, GSH-PX was higher in the 50 kJ m^{-2} UV-B-treated group than the other treatment groups, and at D12, it was 1.08, 1.10, and 1.07 times higher than that of the other three groups, respectively.

3.6. Effects of different doses of UV-B irradiation on CAT, SOD, POD activities and expression of related genes

Changes in CAT and SOD activities during storage of *A. bisporus* are shown in Fig. 6A and Fig. 6C. The overall content of CAT increased slightly at first and then decreased rapidly. At D6 of storage, the CAT activity of the control group was higher than that of the UV-B-treated group; after D12 of storage, the CAT activity of the control group decreased rapidly, whereas that of the UV-B-treated group decreased relatively slowly; at D18 of storage, the CAT activities of the CK, 25 kJ m^{-2} and 100 kJ m^{-2} UV-B-treated groups were 23.40 × 10^3 U kg^{-1}, 18.53 × 10^3 U kg^{-1} and 18.06 × 10^3 U kg^{-1}, which were 70.5 %, 35.1 % and 31.6 % higher than the control group, respectively. In addition, the SOD activity of the UV-B treated group was always higher than that of the control group throughout the storage process, and the 50 kJ m^{-2} UV-B treated group was higher than the other two UV-B treated groups. *CAT2* and *SODc* are genes that regulate the synthesis of CAT and SOD, respectively. From Fig. 6B and Fig. 6D, it can be

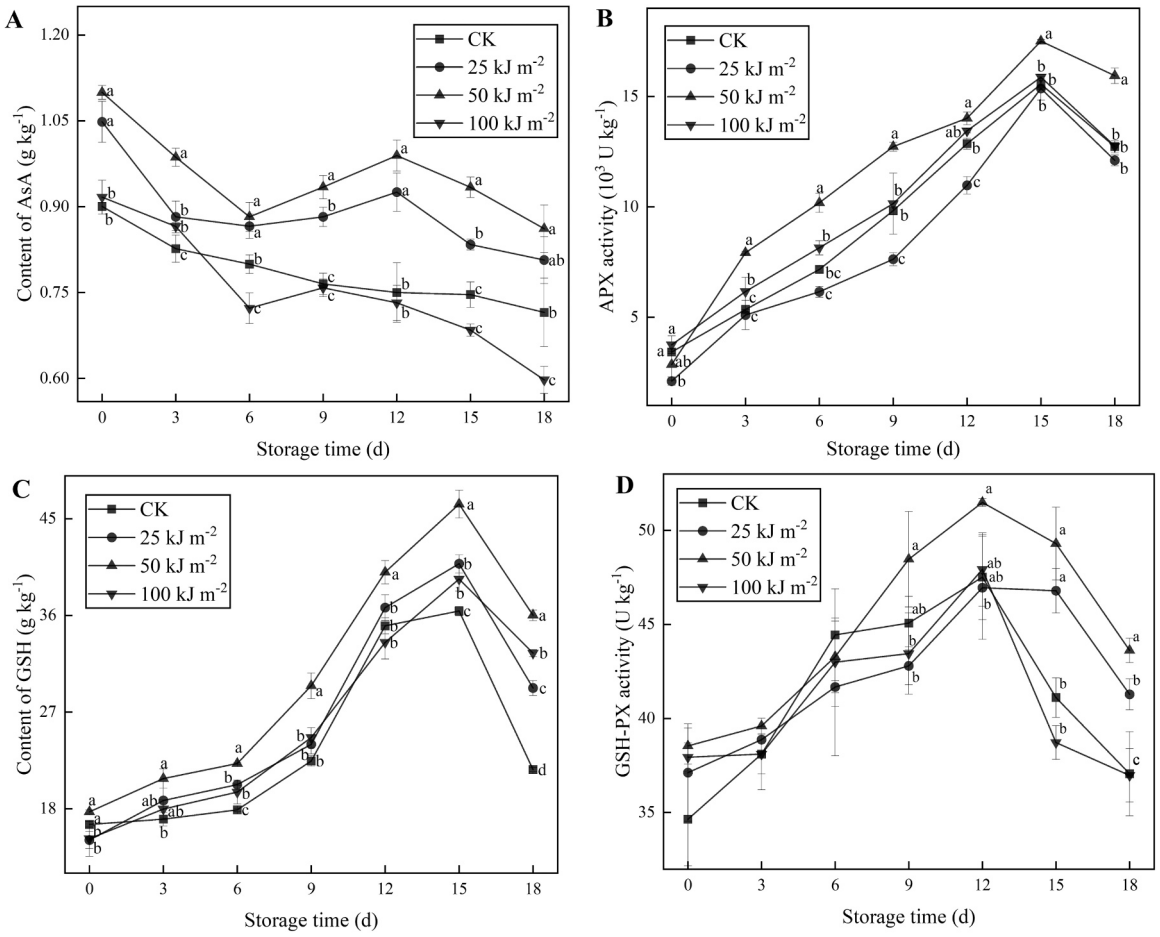

Fig. 5. Effect of different doses of UV-B irradiation on AsA content (A), APX activity (B), GSH content (C), and GSH-PX activity (D) of *A. bisporus.* Dates are expressed as mean ± SD (n = 3). According to Duncan's multiple range test, different lowercase letters indicate significant differences between different treatment groups for the same storage period ($P < 0.05$).

observed that the gene expression of the 50 kJ m^{-2} UV-B-treated group was consistently higher than the other treatment groups throughout the storage process, which was basically consistent with the trend of CAT and SOD.

Guaiacol peroxidase (POD) activity is likewise an important antioxidant enzyme in delaying ROS accumulation (Liu et al., 2014). The POD activity in the 50 kJ m^{-2} UV-B treated group was always higher than that in the control group throughout the storage process, and the highest POD activity was observed at D12, which was 4.02×10^3 U kg^{-1} and 5.67×10^3 U kg^{-1} for the 0 kJ m^{-2} and 50 kJ m^{-2} UV-B treated groups, respectively (Fig. 6E). PrxQ belongs to the Peroxidized Reductase protein Q family, which plays an important role in defense against oxidative stress (Su et al., 2018). With the increase of storage time, the gene expression of *PrxQ* increased and then decreased, and reached the highest peak at D12 (Fig. 6F), with the relative expression of the four groups being 1.05, 1.07, 1.10, and 1.07, respectively. The relative gene expression of *PrxQ* in the 50 kJ m^{-2} UV-B-treated group was higher than the other three groups during the whole storage process. It can be seen that UV-B treatment enhanced the activities of CAT, SOD and POD, and the 50 kJ m^{-2} UV-B treatment had the best effect. This perhaps because the moderate oxidative stress of UV-B promoted the early antioxidant enzyme activities and enhanced the cellular oxidative stress defense capacity thus reducing cellular damage.

Particularly, UVR8 is a plant-specific UV-B photoreceptor (Chen et al., 2022). Fig. 6G showed that UV-B irradiation increased the expression of *UVR8* in *A. bisporus*, and exhibited a tendency of decreasing and then increasing. At D18, the relative expression of *UVR8* in the 50 kJ m^{-2} treatment group reached 1.46, which was higher than the CK group with an expression of 1.08, the result indicated that UV-B radiation could activate the expression of *UVR8*.

3.7. *Effects of different doses of UV-B irradiation on the proliferation and division of peroxisome*

The changes in the relative expression of *PEX5* are shown in Fig. 7A. It can be found that from D9, the expression of the 50 kJ m^{-2} group was lower than that of the CK group and remained low, and at D18, the expression of the four groups was 1.28, 1.29, 1.07, and 1.38, respectively. *PEX11* is an important factor in regulating the division of peroxisomes (Mindthoff et al., 2016), from Fig. 7B, it can be found that the relative expression of *PEX11* basically showed a trend of increasing and then decreasing during the storage process, and the expression levels of the 50 kJ m^{-2} treatment groups were all maintained at a lower level. At D18, the gene expression of the four groups was 1.28, 1.29, 1.07, and 1.38, respectively. Compared with the other three groups, the relative gene expression of the 50 kJ m^{-2} treatment group decreased by 19.86 %, 20.52 % and 29.24 %, respectively.

As shown in Fig. 7C, the relative expression of *PMD1* gradually increased from D3 to D15 and reached a peak at D15, with the expression of 1.15, 1.18, 1.13 and 1.36 in the four groups, respectively, which indicated that after being subjected to the stress of UV-B irradiation, the 50 kJ m^{-2} treatment group delayed peroxisomes proliferation and division compared with the other three groups. This indicates that the peroxisomes in the 50 kJ m^{-2} group maintained a balanced level of

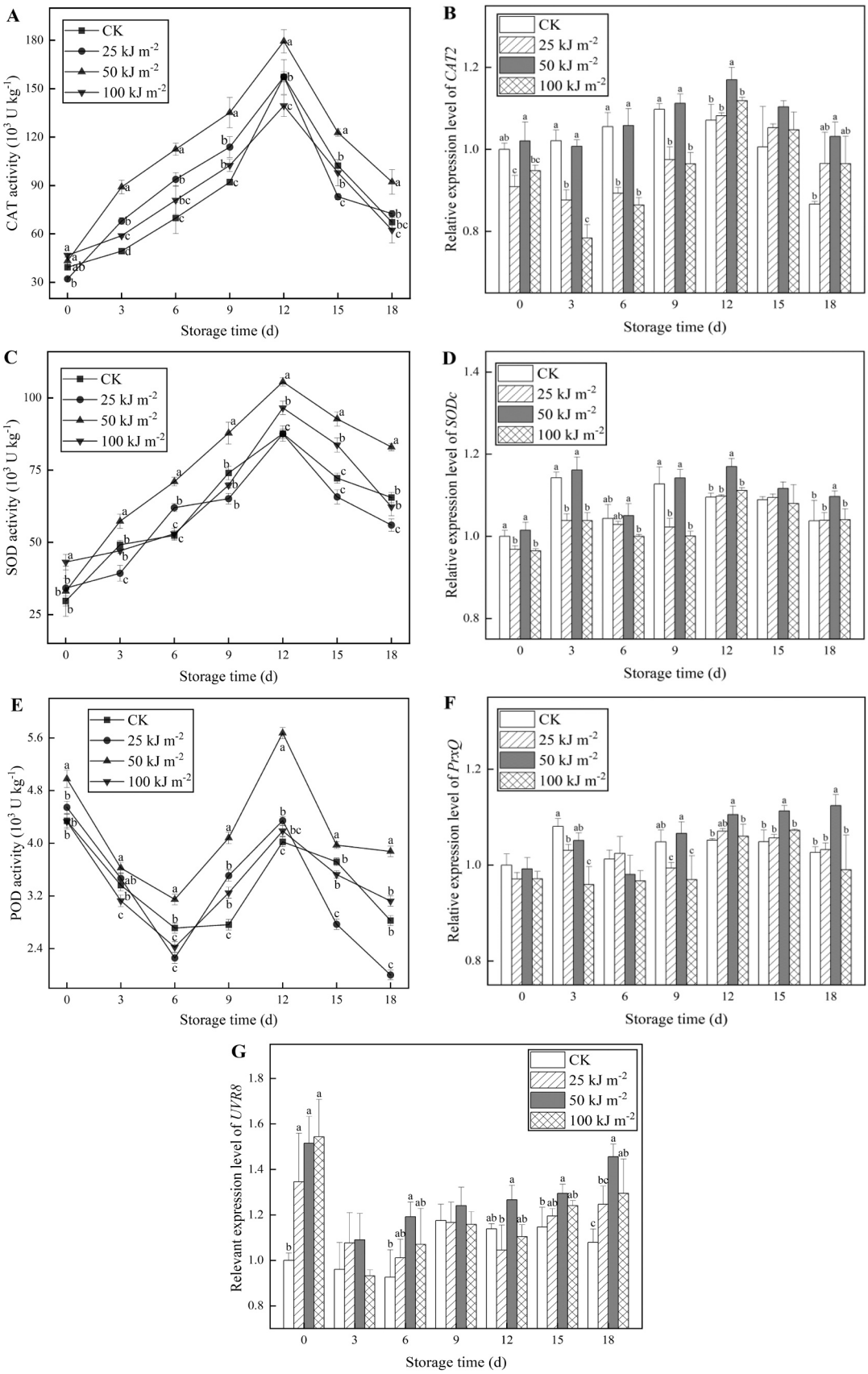

Fig. 6. Effects of different doses of UV-B irradiation on the relative expression of *PXMP2* (A), *PXMP4* (B), *MPV17* (C) and *APO* (D) of *A. bisporus.* Dates are expressed as mean ± SD (n = 3). According to Duncan's multiple range test, different lowercase letters indicate significant differences between different treatment groups for the same storage period ($P < 0.05$).

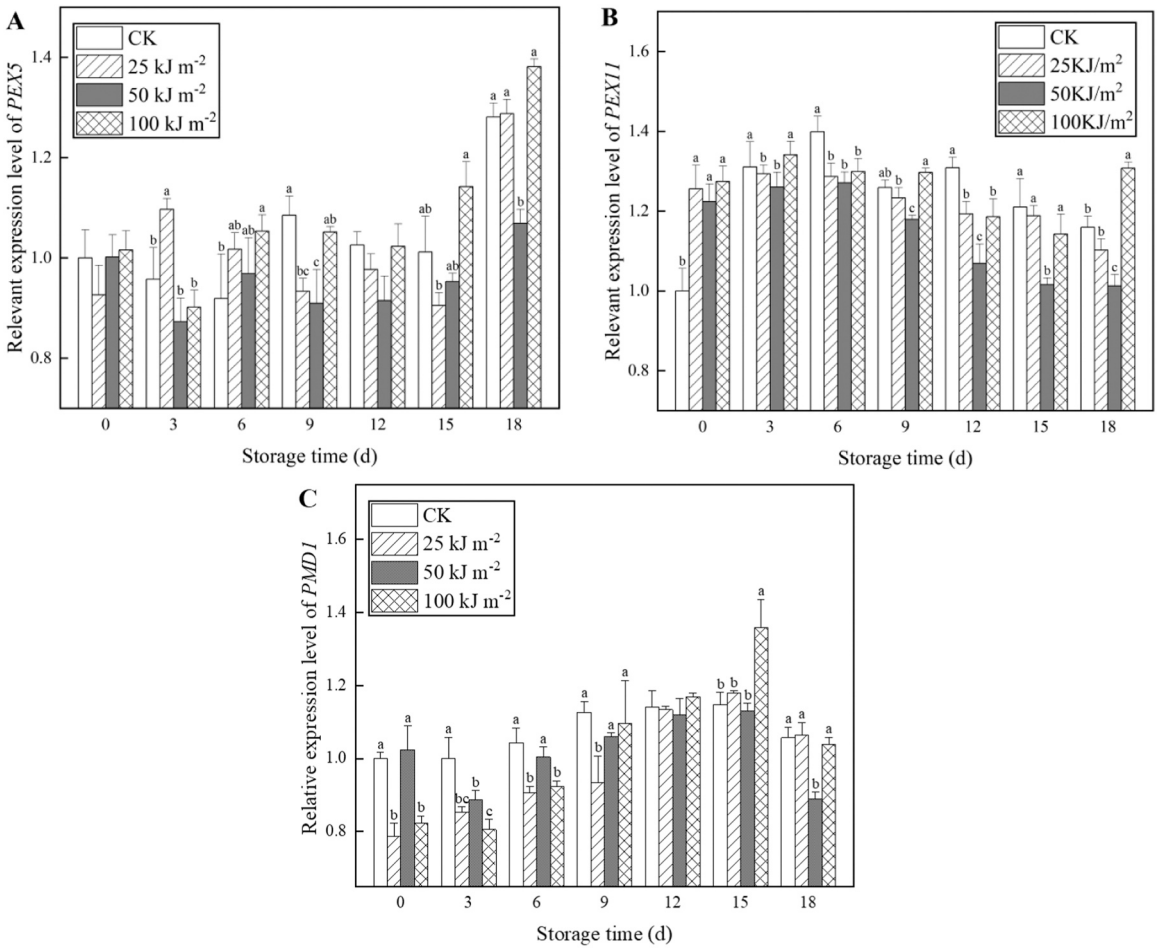

Fig. 7. Effect of different doses of UV-B irradiation on the relative expression of *PEX5* (A), *PEX 11* (B) and *PMD 1* (C) in *A. bisporus*. Dates are expressed as mean ± SD (n = 3). According to Duncan's multiple range test, different lowercase letters indicate significant differences between different treatment groups for the same storage period ($P < 0.05$).

proliferation and autophagy, thus maintaining their metabolic homeostasis.

4. Discussion

4.1. Peroxisomes are important sites for alleviating oxidative stress in postharvest A. bisporus

Peroxisomes contain a variety of enzymes involved in the production and degradation of ROS, which regulate cellular redox homeostasis. The ascorbate-glutathione (AsA-GSH) cycle is an important metabolic pathway of the redox system, and it has been shown to occur in peroxisomes. Romero-Puertas et al. (2006) found the immunocytochemical localization of glutathione reductase (GR) in pea leaf peroxisomes by electron microscopy. Corpas et al. (1994) found the immunocytochemical localization of APX in cucumber cotyledon leaf peroxisomes. Following oxidative stress in organisms, H_2O_2 may be overproduced in the peroxisomal matrix, leading to oxidation of proteins, lipids, metabolites, etc. In the matrix, peroxisomal membranes, and possibly oxidative diffusion to other organelles during transmembrane exposure. Thus, the presence of the AsA-GSH cycle in peroxisomes plays an important role in the maintenance of H_2O_2 as well as redox homeostasis in cells (Reumann and Corpas, 2010). GSH is widely distributed in different subcellular compartments, Ferreira et al. (2023) found that GSH could be transported from the cytosol to peroxisomes by non-selective diffusion. Zechmann and Müller (2008) found 1.7 times higher GSH levels in peroxisomes compared to control cells in pumpkin plants infected with zucchini yellow mosaic virus. Furthermore, H_2O_2 has been widely shown to act as a signaling molecule in different physiological and phytopathological processes. Moreover, H_2O_2 can diffuse freely between organelles and is not only controlled by the compartmentalized function of peroxisomal membranes, but also acts as a signaling molecule in the peroxisomal matrix (Fritz et al., 2007). This suggests that peroxisomes can modulate the body's oxidative stress defense system through H_2O_2, thereby alleviating oxidative stress. PXMP is a widely expressed and abundant homologous peroxisomal membrane protein, and in *A. bisporus* PXMP2, PXMP4 synergistically regulate ROS metabolism and can act as a membrane channel for H_2O_2 (Lismont et al., 2019). Krick et al. (2008) found that Mpv17 prevents mitochondrial oxidative stress and apoptosis through activation of Omi/HtrA2 protease, and that deletion of Mpv17 protein does not affect peroxisome biogenesis, but instead leads to a decreased ability to produce ROS, while overexpression leads to a dramatic increase in intracellular ROS levels. In this study, it was found that when *A. bisporus* was stressed by UV-B irradiation an increase in *MPV17* expression could be detected, which decreased and then increased throughout the storage period, and was lower in the 50 kJ m^{-2} irradiated group than in the CK group, suggesting that 50 kJ m^{-2} UV-B irradiation may have retarded peroxisomal ROS metabolism.

Genes involved in peroxisome formation and proliferation are commonly referred to as the peroxisome functionally regulated protein family PEXs, most of which are involved in the translocation of peroxisomal enzymes to the peroxisome matrix (Kim and Hettema, 2015). Peroxisome matrix proteins contain two intrinsic peroxisome-targeting

signal peptides (PTS, Peroxisome Targeting Signal, PTS1). Most peroxisome matrix proteins, in turn, are transported into the enzyme body mainly through their carried signal peptides and receptor proteins with PEX5 binding to PTS1 of peroxisome proteins in the cytoplasm or PEX7 binding to PTS2 of peroxisome proteins in the cytoplasm before being transported into the enzyme body via the PEX13 and PEX14 docking complexes on the oxisomal membrane (Cross et al., 2016; Skowyra and Rapoport, 2022). Multiple stress conditions induced proliferation of peroxisomes, and it has been shown that PMD1 affects the number and cellular distribution of peroxisomes through cytoskeletal-peroxisomal junctions after exposure to external stress (Frick and Strader, 2018). PEX11 can maintain peroxisome size by triggering peroxisome fission, and the number and size of peroxisomes are closely related to PEX11 protein levels (Galiani et al., 2016; Opaliński et al., 2011). In the present study, *PEX5*, *PEX11* and *PMD1* were found to be at low levels in the 50 kJ m^{-2} group as compared to other treatment groups. This indicates that the peroxisome in the 50 kJ m^{-2} irradiation group maintains a balanced level of proliferation and autophagy, thus maintaining its metabolic homeostasis.

4.2. UV-B irradiation reduces oxidative stress by activating the antioxidant defense system

ROS play a dual role in the response to UV-B which depends on the severity of the stress. When ROS exceed the body's ability to maintain cellular redox homeostasis and exceed the body's ability to scavenge them, it leads to oxidative stress caused by lipid peroxidation, as well as oxidative occurrences of proteins and DNA ultimately leading to structural abnormalities and cellular dysfunction ROS (Gill and Tuteja, 2010). NOX is an important source of ROS production and is known to be involved in responding to ROS production via NADPH oxidase and induced elevated antioxidant enzyme activities in *Arabidopsis* were found by Rao et al. (1996). UV-B irradiation enhanced APX activity in *Arabidopsis* (Haskirli et al., 2021) and POD activity in licorice leaves (Wu et al., 2021). The results of this study showed that $O_2^{\bullet-}$ and H_2O_2 accumulated during postharvest storage of *A. bisporus*. NOX activity and expression of the gene *Rbohf* were suppressed after UV-B irradiation compared to the CK group, they showed an increasing trend in the pre-storage period and were lower than the control when reaching the late storage period. After UV-B irradiation, it could be found that the ROS accumulation in the 50 kJ m^{-2} irradiation treatment group was lower than that in the blank control group, suggesting that UV-B irradiation reduced oxidative stress by decreasing ROS accumulation.

Excess ROS are mainly eliminated by cellular antioxidant systems, including enzymatic antioxidant systems and non-enzymatic antioxidant systems. Enzymatic antioxidant systems, which mainly include CAT, SOD, APX, GSH-PX, etc., these components could reduce the content of intracellular ROS (Wang et al., 2019; Dvořák et al., 2021). SOD detoxifies $O_2^{\bullet-}$, and CAT does so by catabolizing H_2O_2 into H_2O and oxygen. In addition, POD and APX also have antioxidant functions. The ascorbate-glutathione (AsA-GSH) pathway plays a crucial role in detoxifying ROS and interacts with other defense systems and protects the body from oxidative stress damage (Hasanuzzaman et al., 2019). The non-enzymatic antioxidant system mainly consists of substances with reducing capacity, such as ASA, GSH and phenolics (Chirinos et al., 2023). Enhancement of the antioxidant system maintains ROS homeostasis in postharvest fruits, thereby preventing oxidative damage (Huan et al., 2017; Zhang et al., 2018).

Both SOD and CAT enzyme activities were significantly up-regulated after UV-B irradiation, and these increases coincided with the reduction of $O_2^{\bullet-}$ and H_2O_2. Thus, our results suggest that UV-B treatment enhances enzymatic and non-enzymatic antioxidant systems, including SOD, CAT, POD, APX and GSH-PX activities as well as ASA, GSH and phenolic contents to alleviate oxidative stress in postharvest *A. bisporus*. We also investigated the effect of UV-B treatment on SOD and CAT gene expression. As expected, the expression of *SODc* and *CAT2* was significantly elevated in the UV-B irradiation-treated group compared with the control group. Comparable reference could be reported by Chen et al. (2019), who found that up-regulation of the expression of antioxidant systems, such as *SOD*, *CAT*, *GPX*, and *GR*, was up-regulated in the organism of winter wheat by irradiating winter wheat with 10.3 kJ m^{-2} UV-B. Meanwhile, Ma et al. (2019) showed that activation of the antioxidant enzyme systems, such as SOD, CAT, and POD, and the antioxidant enzymes, such as isoflavones, were up-regulated in soybean by UV-B irradiation, enzyme systems as well as non-enzymatic systems such as isoflavones in soybean. Thus, our data suggest that UV-B treatment increases enzyme activities by up-regulating their encoding genes at the transcriptional level. UV-B irradiation may be responsible for the up-regulation of SOD and CAT enzyme functions, which is due to the increase in the transcription of the encoding genes and reduces the accumulation of ROS through the scavenging of $O_2^{\bullet-}$ and H_2O_2, thereby alleviating Oxidative stress.

4.3. UVR8 is a key target for activation of the antioxidant system by UV-B irradiation

UV-B can regulate downstream protein and substance metabolic pathways through induced DNA alterations and its repair mechanisms (Liang et al., 2020). UVR8 is a UV-B receptor responsible for UV-B-triggered signaling in plants (Mishra et al., 2023; Liang et al., 2018), under UV-B irradiation, UVR8 can be converted from a homodimer to a monomer, which triggers the signaling pathway for UV protection (Wu et al., 2012). Its role in photomorphogenesis, acclimation, and UV-B stress tolerance has been well characterized in recent years (Bernula et al., 2017; Liao et al., 2020). It interacts with Constitutively Photomorphogenic 1 (COP1) to initiate UV-B-specific light signaling and regulate UV-B-responsive gene expression, inducing stress protection and repair mechanisms (Favory et al., 2009; Wang et al., 2022). It has been shown that UVR8 is subject to stress-induced gene up-regulation and participates in the phenylpropane pathway to regulate the accumulation of antioxidants such as anthocyanins and flavonoids (Mariz-Ponte et al., 2018). Wu et al. (2016) found that H_2O_2 mediates UV-B-induced anthocyanin biosynthesis in radish sprouts and interacts with UVR8. In addition, Jiang et al. (2022) found that *SlUVR8* was necessary for UV-induced gene expression of *CuZnSOD*, *FeSOD*, and *CAT1*, and that the enhancement of antioxidant enzyme activities was dependent on *SlUVR8*. In the present study, UV-B irradiation was found to significantly activate and efficiently maintain a higher level of *UVR8* expression, this is consistent with the trend of changes in the activity of antioxidant enzymes and the expression of related genes, and thus we inferred that UV-B irradiation activated the *UVR8* receptor in response to UV stress and regulated the downstream antioxidant defense system to delay the oxidative stress damage in postharvest *A. bisporus*. The peroxisome is an important part of the intracellular oxidative defence system. The expression of *PEX5*, *PEX11* and *PMD1* in *A. bisporus* was inhibited by 50 kJ m^{-2} UV-B irradiation, so UVR8 may have a role in regulating the proliferation of peroxisomes. And we mapped the defense mechanism of postharvest *A. bisporus* in response to UV stress by UV-B irradiation in combination with the previous data (Fig. 8). However, the specific regulation of *UVR8* and downstream proteins as well as the interaction between *UVR8* and downstream proteins still need to be investigated.

5. Conclusion

In this study, we further revealed the mechanism of UV-B regulation of oxidative stress defense in postharvest *A. bisporus* by measuring the activities of major enzymes of the antioxidant system, such as CAT, SOD, POD, APX, GSH-PX, and the contents of antioxidant substances, such as AsA and GSH. By exploring the expression levels of key genes for peroxisomal ROS metabolism, we found that 50 kJ m^{-2} UV-B irradiation down-regulated the relative gene expression of *PXMP2*, *PXMP4*, *MPV17*,

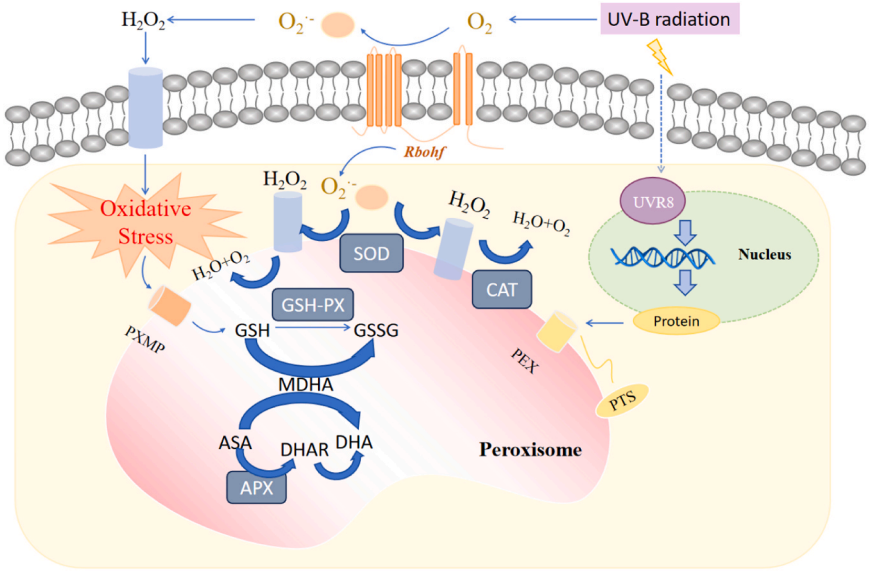

Fig. 8. UV-B irradiation modulates the defence mechanism against oxidative stress in postharvest *A. bisporus*.

and *APO* in *A. bisporus*, which delayed the peroxisomal ROS metabolic pathway, while the relative gene expression of *PEX5*, *PEX11* and *PMD1* in the *A. bisporus* irradiation group was down-regulated at 50 kJ m^{-2} UV-B irradiation. It can be seen that peroxisomes maintained a lower level of proliferation and division, and the accumulation of ROS such as H_2O_2 and $O_2^{\bullet-}$ was reduced. Moreover, 50 kJ m^{-2} UV-B irradiation could effectively induce the activities of key antioxidant enzymes such as CAT, SOD and POD, and up-regulate the expression levels of *UVR8* and antioxidant enzyme-related genes in *A. bisporus*. At the same time, it promotes the AsA-GSH cycle, and increase the accumulation of antioxidant substances such as AsA and GSH, as well as the activities of APX and GSH-PX, which enhance the level of anticorrosive resistance of postharvest *A. bisporus*. In conclusion, moderate UV-B irradiation plays an important role in reducing the damage of postharvest oxidative stress in *A. bisporus* and maintaining cellular redox homeostasis. The role of UVR8 and downstream response factors in the regulation of the peroxisome needs to be further investigated.

CRediT authorship contribution statement

Xueli Shang: Writing – original draft, Formal analysis, Data curation. **Shiqi Bai:** Formal analysis, Data curation. **Liang Wen:** Writing – review & editing. **Alfred Mugambi Mariga:** Investigation. **Ning Ma:** Investigation. **Donglu Fang:** Investigation. **Wenjian Yang:** Investigation. **Qiuhui Hu:** Writing – review & editing. **Fei Pei:** Writing – review & editing, Validation, Methodology, Conceptualization.

Declaration of Competing Interest

The authors declare that they have no known competing financial interests or personal relationships that could have appeared to influence the work reported in this paper.

Acknowledgments

The authors acknowledge financial support from the National Natural Science Foundation of China (32372251), the Outstanding Youth Foundation of Jiangsu Province (BK20240037), Jiangsu Provincial Qinglan Project, Graduate Research Innovation Program of Jiangsu Province (KYCX23_1888), and the Priority Academic Program Development of Jiangsu Higher Education Institutions (PAPD).

Data availability

Data will be made available on request.

References

Bernula, P., Crocco, C., Arongaus, A., Ulm, R., Nagy, F., Viczián, A., 2017. Expression of the UVR8 photoreceptor in different tissues reveals tissue-autonomous features of UV-B signalling. Plant Cell Environ. 40 (7), 1104–1114. https://doi.org/10.1111/pce.12904.

Chapman, J., Muhlemann, J., Gayomba, S., Muday, G., 2019. RBOH-dependent ROS synthesis and ROS scavenging by plant specialized metabolites to modulate plant development and stress responses. Chem. Res. Toxicol. 32 (3), 370–396. https://doi.org/10.1021/acs.chemrestox.9b00028.

Chen, Z., Dong, Y., Huang, X., 2022. Plant responses to UV-B radiation: signaling, acclimation and stress tolerance. Stress Biol. 2, 51. https://doi.org/10.1007/s44154-022-00076-9.

Chen, Z., Ma, Y., Weng, Y., Yang, R., Gu, Z., Wang, P., 2019. Effects of UV-B radiation on phenolic accumulation, antioxidant activity and physiological changes in wheat (*Triticum aestivum L.*) seedlings. Food Biosci. 30, 100409. https://doi.org/10.1016/j.fbio.2019.04.010.

Chirinos, R., Delgado-Pariona, J., Aguilar-Galvez, A., Figueroa-Merma, A., Pacheco-Ávalos, A., Campos, D., Pedreschi, R., 2023. Postharvest storage differentially modulates the enzymatic and non-enzymatic antioxidant system of the exocarp and mesocarp of hass avocado: Implications for disorders. Plants 12 (23), 4008. https://doi.org/10.3390/plants12234008.

Corpas, F., Bunkelmann, J., Trelease, R., 1994. Identification and immunochemical characterization of a family of peroxisome membrane proteins (PMPs) in oilseed glyoxysomes. Eur. J. Cell Biol. 65 (2), 280–290.

Cross, L., Ebeed, H., Baker, A., 2016. Peroxisome biogenesis, protein targeting mechanisms and PEX gene functions in plants. Biochim. Biophys. Acta Mol. Cell Res. 1863 (5), 850–862. https://doi.org/10.1016/j.bbamcr.2015.09.027.

Dokhanieh, A., Aghdam, M., 2016. Postharvest browning alleviation of *Agaricus bisporus* using salicylic acid treatment. Sci. Hortic. 207 (5)), 146–151. https://doi.org/10.1016/j.scienta.2016.05.025.

Dvořák, P., Krasylenko, Y., Zeiner, A., Šamaj, J., Takáč, T., 2021. Signaling toward reactive oxygen species-scavenging enzymes in plants. Front. Plant Sci. 11, 618835. https://doi.org/10.3389/fpls.2020.618835.

Favory, J., Stec, A., Gruber, H., Rizzini, L., Oravecz, A., Funk, M., Albert, A., Cloix, C., Jenkins, G., Oakeley, E., Seidlitz, H., Nagy, F., Ulm, R., 2009. Interaction of COP1 and UVR8 regulates UV-B-induced photomorphogenesis and stress acclimation in *Arabidopsis*. EMBO J. 28, 591–601. https://doi.org/10.1038/emboj.2009.4.

Ferreira, M., Rodrigues, T., Pedrosa, A., Silva, A., Vilarinho, B., Francisco, T., Azevedo, J., 2023. Glutathione and peroxisome redox homeostasis. Redox Biol. 67, 102917. https://doi.org/10.1016/j.redox.2023.102917.

Frick, E., Strader, L., 2018. Kinase MPK17 and the peroxisome division factor PMD1 influence salt-induced peroxisome proliferation. Plant Physiol. 176 (1), 340–351. https://doi.org/10.1104/pp.17.01019.

Fritz, R., Bol, J., Hebling, U., Angermüller, S., Völkl, A., Fahimi, H., Mueller, S., 2007. Compartment-dependent management of H_2O_2 by peroxisomes. Free Radic. Biol. Med. 42, 119–129. https://doi.org/10.1016/j.freeradbiomed.2007.01.014.

Galiani, S., Waithe, D., Reglinski, K., Cruz-Zaragoza, L., Garcia, E., Clausen, M., Schliebs, W., Erdmann, R., Eggeling, C., 2016. Super-resolution microscopy reveals

compartmentalization of peroxisomal membrane proteins. J. Biol. Chem. 291 (33), 16948–16962. https://doi.org/10.1074/jbc.M116.734038.
Gill, S., Tuteja, N., 2010. Reactive oxygen species and antioxidant machinery in abiotic stress tolerance in crop plants. Plant Physiol. Bioch. 48 (12), 909–930. https://doi.org/10.1016/j.plaphy.2010.08.016.
Glady, A., Tanaka, M., Moniaga, C.S., Yasui, M., Hara-Chikuma, M., 2018. Involvement of NADPH oxidase 1 in UVB-induced cell signaling and cytotoxicity in human keratinocytes. Biochem. Biophys. Rep. 14, 7–15. https://doi.org/10.1016/j.bbrep.2018.03.004.
Hasanuzzaman, M., Bhuyan, M., Anee, T., Parvin, K., Nahar, K., Mahmud, J., Fujita, M., 2019. Regulation of ascorbate-glutathione pathway in mitigating oxidative damage in plants under abiotic stress. Antioxidants 8 (9), 384. https://doi.org/10.3390/antiox8090384.
Hasanuzzaman, M., Nahar, K., Anee, T.I., Khan, M., Fujita, M., 2018. Silicon-mediated regulation of antioxidant defense and glyoxalase systems confers drought stress tolerance in *Brassica napus* L. S. Afr. J. Bot. 115, 50–57. https://doi.org/10.1016/j.sajb.2017.12.006.
Haskirli, H., Yilmaz, O., Ozgur, R., Uzilday, B., Turkan, I., 2021. Melatonin mitigates UV-B stress via regulating oxidative stress response, cellular redox and alternative electron sinks in Arabidopsis thaliana. Phytochemistry 182, 112592. https://doi.org/10.1016/j.phytochem.2020.112592.
Huan, C., Han, S., Jiang, L., An, X., Yu, M., Xu, Y., Ma, R., Yu, Z., 2017. Postharvest hot air and hot water treatments affect the antioxidant system in peach fruit during refrigerated storage. Postharvest Biol. Technol. 126, 1–14. https://doi.org/10.1016/j.postharvbio.2016.11.018.
Jiang, Z., Xu, M., Dong, J., Zhu, Y., Lou, P., Han, Y., Hao, J., Yang, Y., Ni, J., Xu, M., 2022. UV-B pre-irradiation induces cold tolerance in tomato fruit by SlUVR8-mediated upregulation of superoxide dismutase and catalase. Postharvest Biol. Technol. 185, 111777. https://doi.org/10.1016/j.postharvbio.2021.111777.
Kim, P., Hettema, E., 2015. Multiple pathways for protein transport to peroxisomes. J. Mol. Bio. 427 (6), 1176–1190. https://doi.org/10.1016/j.jmb.2015.02.005.
Krick, S., Shi, S., Ju, W., Faul, C., Tsai, S., Mundel, P., Böttinger, E., 2008. Mpv17l protects against mitochondrial oxidative stress and apoptosis by activation of Omi/HtrA2 protease. Proc. Natl. Acad. Sci. 105 (37), 14106–14111. https://doi.org/10.1073/pnas.0801146105.
Li, T., Yamane, H., Tao, R., 2021. Preharvest long-term exposure to UV-B radiation promotes fruit ripening and modifies stage-specific anthocyanin metabolism in highbush blueberry. Hortic. Res. 8 (1), 67. https://doi.org/10.1038/s41438-021-00503-4.
Liang, T., Shi, C., Peng, Y., Tan, H., Xin, P., Yang, Y., Wang, F., Li, X., Chu, J., Huang, J., Yin, Y., Liu, H., 2020. Brassinosteroid-activated BRI1-EMS-SUPPRESSOR 1 inhibits flavonoid biosynthesis and coordinates growth and UV-B stress responses in plants. Plant Cell 32 (10), 3224–3239. https://doi.org/10.1105/tpc.20.00048.
Liang, T., Yang, Y., Liu, H., 2018. Signal transduction mediated by the plant UV-B photoreceptor UVR8. N. Phytol. 211 (3), 1247–1252. https://doi.org/10.1111/nph.15469.
Liao, X., Liu, W., Yang, H., Jenkins, G., 2020. A dynamic model of UVR8 photoreceptor signalling in UV-B-acclimated *Arabidopsis*. N. Phytol. 227 (3), 857–866. https://doi.org/10.1111/nph.16581.
Lin, M., Huang, Y., Orihara, K., Chibana, H., Kajiwara, S., Chen, X., 2024. A putative NADPH oxidase gene in unicellular pathogenic *Candida glabrata* is required for fungal ROS production and oxidative stress response. J. Fungi. 10 (1), 16. https://doi.org/10.3390/jof10010016.
Lismont, C., Koster, J., Provost, S., Baes, M., Veldhoven, P., Waterham, H., Fransen, M., 2019. Deciphering the potential involvement of PXMP2 and PEX11B in hydrogen peroxide permeation across the peroxisomal membrane reveals a role for PEX11B in protein sorting. Biochim. Biophys. Acta Biomembr. 1861 (10), 182991. https://doi.org/10.1016/j.bbamem.2019.05.013.
Liu, J., Wu, Y., Kan, J., Wang, Y., Jin, C., 2013. Changes in reactive oxygen species production and antioxidant enzyme activity of *Agaricus bisporus* harvested at different stages of maturity. J. Sci. Food Agric. 93, 2201–2206. https://doi.org/10.1002/jsfa.6027.
Liu, N., Lin, Z., Guan, L., Gaughan, G., Lin, G., 2014. Antioxidant enzymes regulate reactive oxygen species during pod elongation in *Pisum sativum* and *Brassica chinensis*. PLoS One 9 (2), e87588. https://doi.org/10.1371/journal.pone.0087588.
Ma, M., Wang, P., Yang, R., Zhou, T., Gu, Z., 2019. UV-B mediates isoflavone accumulation and oxidative-antioxidant system responses in germinating soybean. Food Chem. 275, 628–636. https://doi.org/10.1016/j.foodchem.2018.09.158.
Mariz-Ponte, N., Mendes, R., Sario, S., Ferreira de Oliveira, J., Melo, P., Santos, C., 2018. Tomato plants use non-enzymatic antioxidant pathways to cope with moderate UV-A/B irradiation: A contribution to the use of UV-A/B in horticulture. J. Plant Physiol. 221, 32–42. https://doi.org/10.1016/j.jplph.2017.11.013.
Mindthoff, S., Grunau, S., Steinfort, L., Girzalsky, W., Hiltunen, J., Erdmann, R., Antonenkov, V., 2016. Peroxisomal Pex11 is a pore-forming protein homologous to TRPM channels. Biochim. Biophys. Acta Mol. Cell Res. 1863 (2), 271–283. https://doi.org/10.1016/j.bbamcr.2015.11.013.
Mishra, V., Singh, S., Dubey, N., Singh, S., Rai, M., Tripathi, D., Singh, V., 2023. How is UVR8 relevant in plants? New evidence. Plant Growth Regul. 100, 1–5. https://doi.org/10.1007/s10725-022-00939-1.
Opaliński, Ł., Kiel, J., Williams, C., Veenhuis, M., van der Klei, I., 2011. Membrane curvature during peroxisome fission requires Pex11. EMBO J. 30 (1), 5–16. https://doi.org/10.1038/emboj.2010.299.
Rao, M., Paliyath, G., Ormrod, D.P., 1996. Ultraviolet-B-and ozone-induced biochemical changes in antioxidant enzymes of *Arabidopsis thaliana*. Plant Physiol. 110, 125–136. https://doi.org/10.1104/pp.110.1.125.
Reumann, S., Corpas, F., 2010. The Peroxisomal Ascorbate–Glutathione Pathway: molecular identification and insights into its essential role under environmental stress conditions. Ascorbate-Glutathione Pathw. Stress Toler. Plants 387–404. https://doi.org/10.1007/978-90-481-9404-9_14.
Romero-Puertas, M., Corpas, F., Sandalio, L., Leterrier, M., Rodríguez-Serrano, M., Del Río, L., Palma, J., 2006. Glutathione reductase from pea leaves: response to abiotic stress and characterization of the peroxisomal isozyme. N. Phytol. 170, 43–52. https://doi.org/10.1111/j.1469-8137.2005.01643.x.
Santin, M., Lucini, L., Castagna, A., Chiodelli, G., Hauser, M.-T., Ranieri, A., 2018. Post-harvest UV-B radiation modulates metabolite profile in peach fruit. Postharvest Biol. Technol. 139, 127–134. https://doi.org/10.1016/j.postharvbio.2018.02.001.
Sheng, K., Shui, S., Yan, L., Liu, C., Zheng, L., 2018. Effect of postharvest UV-B or UV-C irradiation on phenolic compounds and their transcription of phenolic biosynthetic genes of table grapes. J. Food Sci. Technol. 55, 3292–3302. https://doi.org/10.1007/s13197-018-3264-1.
Shoaib, N., Pan, K., Mughal, N., Raza, A., Liu, L., Zhang, J., Wu, X., Sun, X., Zhang, L., Pan, Z., 2024. Potential of UV-B radiation in drought stress resilience: A multidimensional approach to plant adaptation and future implications. Plant Cell Environ. 47, 387–407. https://doi.org/10.1111/pce.14774.
Skowyra, M., Rapoport, T., 2022. PEX5 translocation into and out of peroxisomes drives matrix protein import. Mol. Cell. 82 (17), 3209–3225. https://doi.org/10.1016/j.molcel.2022.07.004.
Su, T., Si, M., Zhao, Y., Liu, Y., Yao, S., Che, C., Chen, C., 2018. A thioredoxin-dependent peroxiredoxin Q from *Corynebacterium glutamicum* plays an important role in defense against oxidative stress. Plos One 13 (2), e0192674. https://doi.org/10.1371/journal.pone.0192674.
Usall, J., Ippolito, A., Sisquella, M., Neri, F., 2016. Physical treatments to control postharvest diseases of fresh fruits and vegetables. Postharvest Biol. Technol. 122, 30–40. https://doi.org/10.1016/j.postharvbio.2016.05.002.
Vidović, M., Morina, F., Milić, S., Albert, A., Zechmann, B., Tosti, T., Winkler, J., Jovanović, S., 2015. Carbon allocation from source to sink leaf tissue in relation to flavonoid biosynthesis in variegated *Pelargonium zonale* under UV-B radiation and high PAR intensity. Plant Physiol. Bioch. 93, 44–55. https://doi.org/10.1016/j.plaphy.2015.01.008.
Wang, L., Wang, C., Liu, X., Cheng, J., Li, S., Zhu, J., Gong, Z., 2019. Peroxisomal β-oxidation regulates histone acetylation and DNA methylation in *Arabidopsis*. Proc. Natl. Acad. Sci. 116 (21), 10576–10585. https://doi.org/10.1073/pnas.1904143116.
Wang, Y., Wang, L., Guan, Z., Chang, H., Ma, L., Shen, C., Qiu, L., Yan, J., Zhang, D., Li, J., Deng, X., Yin, P., 2022. Structural insight into UV-B-activated UVR8 bound to COP1. Sci. Adv. 8 (16), eabn3337. https://doi.org/10.1126/sciadv.abn3337.
Wang, Y., Wei, X., Jing, X., Chang, Y., Hu, C., Wang, X., Chen, K., 2016. The fundamental role of NOX family proteins in plant immunity and their regulation. Int. J. Mol. Sci. 17 (6), 805. https://doi.org/10.3390/ijms17060805.
Wu, D., Hu, Q., Yan, Z., Chen, W., Yan, C., Huang, X., Zhang, J., Yang, P., Deng, H., Wang, J., Deng, X., Shi, Y., 2012. Structural basis of ultraviolet-B perception by UVR8. Nature 484 (7393), 214–219. https://doi.org/10.1038/nature10931.
Wu, Q., Su, N., Zhang, X., Liu, Y., Cui, J., Liang, Y., 2016. Hydrogen peroxide, nitric oxide and UV RESISTANCE LOCUS8 interact to mediate UV-B-induced anthocyanin biosynthesis in radish sprouts. Sci. Rep. 6, 29164. https://doi.org/10.1038/srep29164.
Wu, S., Yu, K., Ding, X., Song, F., Liang, X., Li, Z., Peng, L., 2021. Transcriptomic analyses reveal dynamic changes of defense response in *Glycyrrhiza uralensis* leaves under enhanced ultraviolet-B radiation. Plant Physiol. Biochem. 163, 358–366. https://doi.org/10.1016/j.plaphy.2021.04.010.
Wu, X., Zhang, S., Li, X., Zhang, F., Fan, Y., Liu, Q., Wan, X., Lin, T., 2021. Postharvest UV-B radiation increases enzyme activity, polysaccharide and secondary metabolites in honeysuckle (*Lonicera japonica* Thunb.). Ind. Crops Prod. 171, 113907. https://doi.org/10.1016/j.indcrop.2021.113907.
Yokawa, K., Baluška, F., 2015. Pectins, ROS homeostasis and UV-B responses in plant roots. Phytochemistry 112, 80–83. https://doi.org/10.1016/j.phytochem.2014.08.016.
Zechmann, B., Müller, M., 2008. Effects of zucchini yellow mosaic virus infection on the subcellular distribution of glutathione and its precursors in a highly tolerant *Cucurbita pepo* cultivar. Botany 86 (9), 1092–1100. https://doi.org/10.1139/B08-048.
Zhang, H., He, H., Song, W., Zheng, L., 2023. Pre-harvest UVB irradiation enhances the phenolic and flavonoid content, and antioxidant activity of green- and red-leaf lettuce cultivars. Horticulturae 9 (6), 695. https://doi.org/10.3390/horticulturae9060695.
Zhang, K., Pu, Y., Sun, D., 2018. Recent advances in quality preservation of postharvest mushrooms (*Agaricus bisporus*): a review. Trends Food Sci. Tech. 78, 72–82. https://doi.org/10.1016/j.tifs.2018.05.012.
Zhang, Y., Huber, D., Hu, M., Jiang, G., Gao, Z., Xu, X., Jiang, Y., Zhang, Z., 2018. Delay of postharvest browning in litchi fruit by melatonin via the enhancing of antioxidative processes and oxidation repair. J. Agric. Food Chem. 66 (28), 7219–7552. https://doi.org/10.1021/acs.jafc.8b01922.